Fluctuations in Late Pennsylvanian (Virgilian) seawater chemistry inferred from submarine cements of phylloid algal mounds, western Orogrande Basin (New Mexico)

Shane C. Seals, Gerilyn S. Soreghan, and R. D. Elmore

2002, pp. 167-177. https://doi.org/10.56577/FFC-53.167

in:

Geology of White Sands, Lueth, Virgil; Giles, Katherine A.; Lucas, Spencer G.; Kues, Barry S.; Myers, Robert G.; Ulmer-Scholle, Dana; [eds.], New Mexico Geological Society 53rd Annual Fall Field Conference Guidebook, 362 p. https://doi.org/10.56577/FFC-53

This page is intentionally left blank to maintain order of facing pages.

New Mexico Geological Society Guidebook, 53rd Field Conference, Geology of White Sands, 2002, p. 167-177.

FLUCTUATIONS IN LATE PENNSYLVANIAN (VIRGILIAN) SEAWATER CHEMISTRY INFERRED FROM SUBMARINE CEMENTS OF PHYLLOID ALGAL MOUNDS, WESTERN OROGRANDE BASIN (NEW MEXICO)

SHANE C. SEALS, GERILYN S. SOREGHAN AND R. D. ELMORE

School of Geology and Geophysics, University of Oklahoma, 810 SEC, 100 E. Boyd St., Norman, OK 73019

Abstract.—Reworked clasts of submarine cements exhibiting fine fabric preservation occur within a thin (20 cm), shale-encased lithoclastic packstone present in the proximal mound flank of a phylloid algal mound complex from the western Orogrande basin (New Mexico). Mounds within this complex contain abundant recrystallized submarine cement in mound-core cementstone and foraminiferal/algal boundstone facies. Volumetrically abundant cementstone is particularly prevalent at the bases of high-frequency (glacioeustatic) sequences, while foraminiferal/algal boundstone typically occurs at the tops of sequences. Although in situ submarine cement within the mound core is uniformly recrystallized, clasts of finely preserved (radial-fibrous) submarine cement occur within a lithoclastic packstone unit adjacent to the mound core. Here, we report on the optical and chemical properties of both in situ, recrystallized submarine cement from mound-core units and transported clasts of fabric-retentive cement preserved within the mound-flank unit.

Three cement types are observed as clasts within the lithoclastic packstone unit. Type 1 cement characterizes clasts derived from nonfossiliferous cementstone. It is radial-fibrous, light brown, and exhibits sweeping extinction. Solid inclusions of magnetite and/or pyrrhotite, and hematite line radial growth fronts within this cement type. Microprobe analysis indicates overall low Fe, Mn, and Mg and moderately elevated Sr with locally high Fe and Mn. Type 2 cement occurs within clasts of foraminiferal/algal boundstones; it is also radial-fibrous, light brown, and exhibits abundant sweeping extinction. In contrast to the type 1 cement, however, this cement lacks Fe-rich growth bands, and exhibits zones of fluctuating Mg concentration. Low-Mg zones ($\leq$ 1000 ppm) contain low Fe and Mn and high Sr. High-Mg zones (> 4000 ppm) exhibit moderate Fe, variable Mn, and relatively depleted Sr. Type 3 cement consists entirely of recrystallized, sparry calcite fans which are colorless to light brown, non-pleochroic, and contain low Fe, Mn, and Mg and variable Sr. Type 1 and 2 cements occur only within transported clasts of the studied lithoclastic packstone, whereas type 3 cement occurs as clasts within the packstone and within basal-sequence cementstones of the mound core.

Optical properties and trace element chemistry of all the cement types indicate pseudomorphism of an aragonite precursor. We infer that type 1 cement was derived from *in situ* cementstone formed in basal sequence positions within the mound core. Solid inclusions of Fe-rich phases within this cement together with the lack of biota suggest precipitation under oxygen-poor conditions likely associated with onset of glacioeustatic transgressions. In contrast, abundant biota and lack of Fe-rich inclusions in the type-2 cement of foraminiferal/algal boundstone indicates oxic conditions. These data suggest that seawater chemistry within the Late Pennsylvanian Orogrande basin evolved from oxygen-poor during early transgressions to oxygen-rich at highstands through glacioeustatic cycles.

INTRODUCTION

Submarine cements are well documented in many ancient and modern marine systems (e.g., Shinn, 1969; Davies, 1977; Wendt, 1977; Assereto and Folk, 1980; Kimbell and Humphrey, 1994; Grotzinger and Knoll, 1995; Woods et al., 1999; Nelson and James, 2000), and the primary mineralogy of such cements has fluctuated between calcite-dominant and aragonite dominant over Phanerozoic time (MacKenzie and Pigott, 1981; Sandberg, 1983). The Late Paleozoic was characterized by aragonite seafloor precipitates and cements in algal bioherms (e.g., Bathurst, 1959; Davies, 1977; Mazzullo and Cys, 1979; Wahlman, 1985, 1988; Davies and Nassichuk, 1990; Rahnis and Kirkland, 1999). Pennsylvanian-Lower Permian phylloid algal bioherms crop out at several localities along the margins of the Orogrande basin of southern New Mexico (Fig. 1), are well exposed and have been well studied along the eastern Sacramento shelf (Fig. 2, e.g., Plumley and Graves, 1953; Wray, 1962; Otte and Parks, 1963; Cys and Mazzullo, 1977; Toomey et al., 1977; Wilson, 1977; Mazzullo and Cys, 1979; Pol, 1982, 1985; Toomey and Babcock, 1983; Goldstein, 1988; Wahlman et al., 1992; Gordon, 1997; Stoklosa et al., 1998). Large, well-exposed phylloid algal bioherms along the western margin of the Orogrande basin have until recently remained poorly studied because of limited access to the U.S. Army White Sands Missile Range (Kottlowski et al., 1956; Soreghan and Giles, 1999a; Soreghan et al., 2000; Doherty et al., 2002). These phylloid algal bioherms were deposited within thick sequences of mixed shallow-marine carbonate and siliciclastic strata, which record high-frequency cyclicity related to large-magnitude glacioeustatic sea level fluctuations (Soreghan and Giles, 1999a,b). Thus, the marine chemistry of Pennsylvanian oceans should exhibit an unusual character. In this paper we present petrographic, geochemical, and rock magnetic analyses of both recrystallized and well-preserved submarine cements present within the mound system of the western Orogrande basin. These cements exhibit ranges in texture and chemistry that suggest that seawater chemistry evolved through the course of glacioeustatic (high-frequency) sequences.

UPPER CARBONIFEROUS ALGAL MOUNDS OF THE WESTERN OROGRANDE BASIN

Along the western margin of the Orogrande basin, large ($\geq$ 130 m thick) pinnacle-like phylloid algal mounds occur in the Upper Pennsylvanian (Virgilian) Panther Seep Formation (Fig. 3) and are exposed over a 20 km^2 region in Hembrillo Canyon of the San Andres Mountains. These algal mounds contain volumetrically abundant submarine cement in mound-core boundstone and cementstone facies (Soreghan and Giles, 1999a). These mounds were first documented by Kottlowski et al. (1956), and have

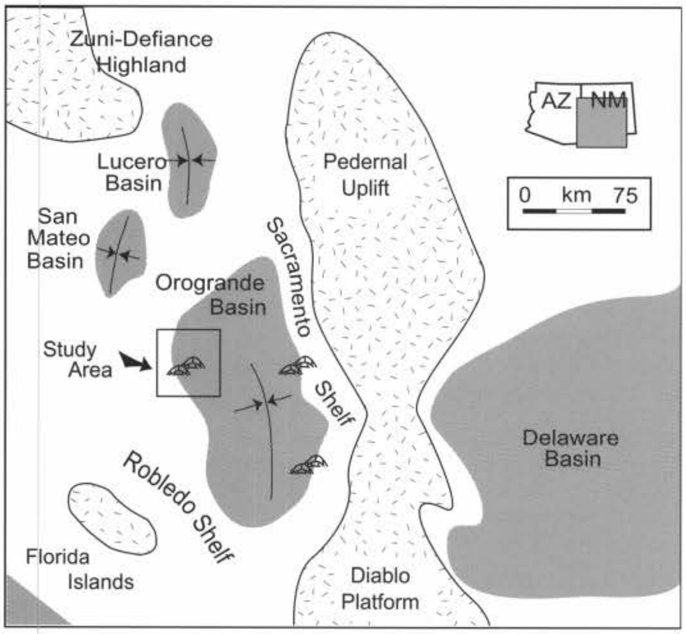

FIGURE 1. Late Pennsylvanian-Early Permian paleogeographic map of southwestern extent of the Ancestral Rocky Mountains, showing basins and topographic highs. Phylloid algal mounds developed along the periphery of the basin to the east (Sacramento Mountains), southeast (Hueco Mountains), and to the west (San Andres Mountains). Modified from Soreghan and Giles (1999a).

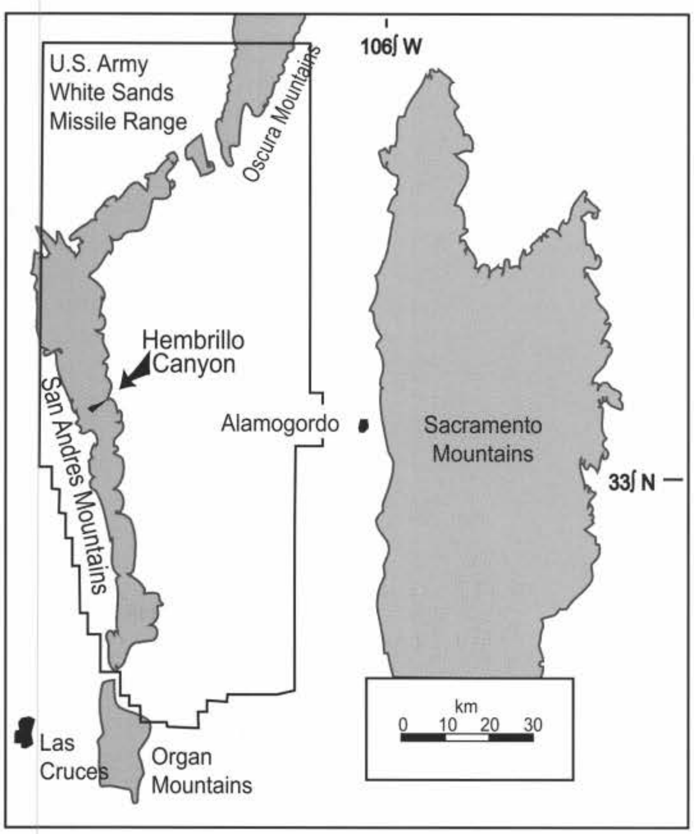

FIGURE 2. Regional location map showing area of Hembrillo Canyon. Modified from Soreghan and Giles (1999a).

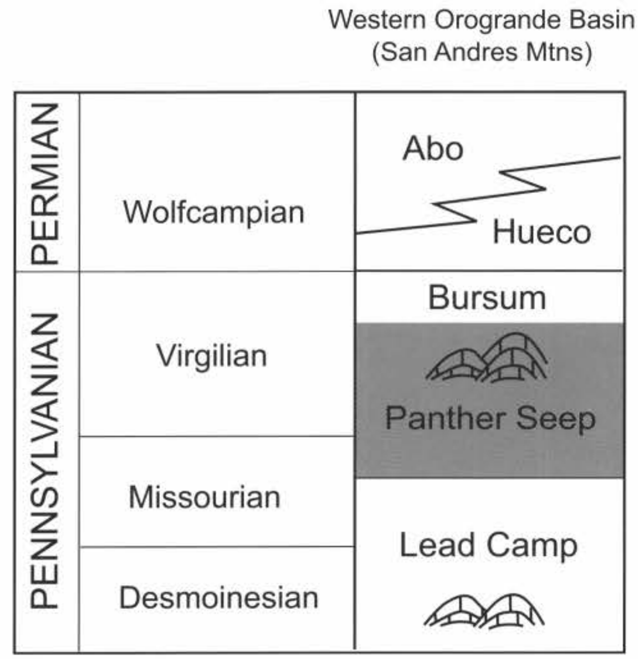

FIGURE 3. Pennsylvanian-Permian stratigraphy of the western Orogrande basin. Phylloid algal mounds crop out in the Panther Seep Formation (this study) and Lead Camp Formation (both located in the San Andres Mountains). After Kottlowski et al. (1956).

recently received more detailed study by Soreghan and Giles (1999a,b), Soreghan et al. (2000), and Doherty et al. (2002).

Three general facies occur within the mound system (Soreghan and Giles, 1999a), (1) mound-core facies, (2) mound-flank facies, and (3) off-mound facies. The mound-core facies consist predominantly of cementstone, phylloid-algal, foraminiferal-algal, and algal-peloidal boundstone, and intermixed wackestone and packstone facies. Single depositional sequences within the mound-core range up to 40 m thick (average 15 m) and are capped by exposure surfaces (sequence boundaries). These high-frequency sequences are the result of high-amplitude glacioeustasy (Soreghan and Giles, 1999a,b) that operated throughout Pennsylvanian-Early Permian time. Mound-flank and off-mound facies commonly display evidence of shallowing prior to exposure. Mound-flank depositional sequences are on average 7.5 m thick, and can range up to 20 m thick. Mound-flank sequences consist of a basal skeletal wackestone overlain by boundstone facies. The boundstone are commonly capped by dolomitized packstone facies truncated ultimately by subaerial exposure surfaces. Off-mound depositional sequences are generally thin (< 8 m) and consist of oncoidal wackestone and silty carbonate overlain by subtidal packstone and dolomitized peritidal facies.

Stratiform dolomitization preferentially affects peritidal facies and strata proximal to sequence boundaries (Soreghan et al., 2000). Soreghan et al. (2000) described two replacive dolomite phases, facies selective (FS) and non-facies selective (NFS), which constitute 95% of the dolomite in the mound system, and several early dolomitic cements. FS dolomite is finely crystalline, fabric-retentive dolomite that occurs only in the peritidal facies and has elevated Sr and Na and low to moderate Fe and

Mn. FS dolomite was formed penecontemporaneously with peritidal deposition during glacioeustatic sea level fall and lowstand (Soreghan et al., 2000). NFS dolomite is medium- to coarse-grained and contains locally elevated Sr and Na, and moderate to high Fe and Mn. NFS dolomite increases in abundance towards the tops of glacioeustatic sequences and is interpreted as the result of reflux of mesosaline water during early transgressions (Soreghan et al., 2000).

METHODS

Samples of a lithoclastic packstone unit containing clasts of submarine cement were collected from the flank of a high-relief (> 130 m), well-exposed phylloid algal mound complex in Hembrillo Canyon and compared to samples of *in situ* cementstone collected from the mound core. Several standard and polished thin sections were stained with a potassium ferricyanide alizarin red-S solution (Dickson, 1965) and analyzed using transmitted and reflected light, and cathodoluminescence (Cambridge Image Technology Ltd. CLmk4 cathodoluminoscope, CL). Morphologic and textural contrasts among the different cement types preserved in the lithoclastic packstone were analyzed on a single polished thin section using scanning electron microscopy (SEM). Major and minor elemental constituents, including Fe, Mg, Mn, and Sr, were determined for each of the cement types by quantitative electron probe microanalysis (QEPMA) using a Cameca SX-50 electron microprobe at the University of Oklahoma. Analyses of minerals were conducted at 10 nA and, 20 kV, using a spot size of 20 μm, and counting times of 45 seconds for all minerals. For typical concentrations of study samples precision is $\pm$ 39 ppm for Mg, $\pm$ 52 ppm for Fe, $\pm$ 75 ppm for Mn, and $\pm$48 ppm for Sr. Minimum detection limits for Mg, Fe, Mn, and Sr are 108 ppm, 245 ppm, 209 ppm, and 385 ppm, respectively. Owing to the difficulty in distinguishing the mineralogy of Fe-rich inclusions present in the type 1 cement using either microprobe (BSE) or petrographic approaches; we employed rock-magnetic analyses on bulk rock cores. Eleven standard-size (2.5 cm diameter, 3 cm length) cores were drilled from an oriented sample of the lithoclastic packstone unit using a gasoline-powered drill. The natural remanent magnetizations (NRMs) of specimens were measured on a 2G three-axes cryogenic magnetometer located in a magnetically shielded room. Several specimens were also subjected to alternating field (AF) demagnetization up to 120 mT in a 2G Automated Degaussing System. An impulse magnetizer was used to obtain the acquisition pattern of an isothermal remanent magnetization (IRM) and was followed by thermal decay in a stepwise fashion up to 700ºC in an Schonstedt TSD-1 oven of three perpendicular IRMs (Lowrie, 1990) with fields of 120 mT, 500 mT, and 2500 mT.

DEPOSITIONAL CONTEXT OF THE SUBMARINE CEMENTS

Various types of cements occur within Upper Carboniferous phylloid algal bioherms of the western Orogrande basin. Facies at sequence bases typically consist entirely of cementstones devoid of any macroscopic biota. The cement appears to have been a direct sea floor precipitate that composed the mound structure prior to colonization by various organisms, such as phylloid and dasycladaceaen algae (Soreghan and Giles, 1999a). Sequence tops typically contain fibrous, recrystallized *in situ* cement within algal and foraminiferal boundstone (Soreghan and Giles, 1999a).

In contrast to *in situ* cements present in mound-core facies, abraded clasts of well-preserved fibrous cements occur within a thin (< 20 cm thick) lithoclastic packstone unit proximal to the mound flank (Figs. 4a,b). Nowhere else within the mound system have these well-preserved cements been observed. The studied lithoclastic packstone is bounded above and below by shale and is thickest proximal to the mound-flank and wedges toward both the mound-core and distal flank (Figs. 4a,b). This unit contains abraded lithoclasts of cementstone, boundstone, and packstone composed of or containing early-precipitated submarine cement.

Debris preserved within the studied lithoclastic packstone was eroded from the mound system and transported short distances. Because of its occurrence near the base of a glacioeustatic cycle (Fig. 4b) the lithoclastic packstone incorporates material eroded from various parts (transgressive highstand) of the underlying cycle possibly, in addition to material eroded penecontemporaneously from the topographically higher mound core. Material eroded from topographically high parts of the underlying cycle apparently underwent meteoric diagenesis and recrystallization before incorporation into the lithoclastic packstone, but other clasts survived in pristine condition. Relatively thick (> 1 m) shale encasing the lithoclastic packstone likely acted as an aquitard allowing the unique preservation within the unit.

SUBMARINE CEMENTS OF THE WESTERN OROGRANDE MOUNDS

In situ Mound-Core Cements

Cementstones collected *in situ* from the bases of mound-core sequences consist of recrystallized faintly radial-fibrous sparry calcite mosaics that are clear to light brown in color, and non-pleochroic. Microprobe analysis on these *in situ* mound-core cements reveals low concentrations of Mg (1430 ppm $\pm$ 390), Fe and Mn below detection limit (BDL), and generally low but slightly varying concentrations of Sr (510 ppm $\pm$ 300) ranging from 1400 ppm to BDL as compared to other ancient rocks (Tucker and Wright, 1990). The faintly radial-fibrous texture, and locally elevated concentrations of Sr are consistent with an aragonitic precursor. Also, these characteristics closely resemble those described by previous authors (Otte and Parks, 1963; Cys and Mazzullo, 1977; Mazzullo and Cys, 1979) for former aragonitic botryoids from mounds of the eastern Orogrande basin.

Cement Clasts Preserved in the Lithoclastic Packstone

On the basis of petrographic and geochemical analysis of clasts within the lithoclastic packstone we recognize three distinct types of cement. These include (1) radial-fibrous cement in cementstone facies, (2) radial-fibrous cement in boundstone facies, and

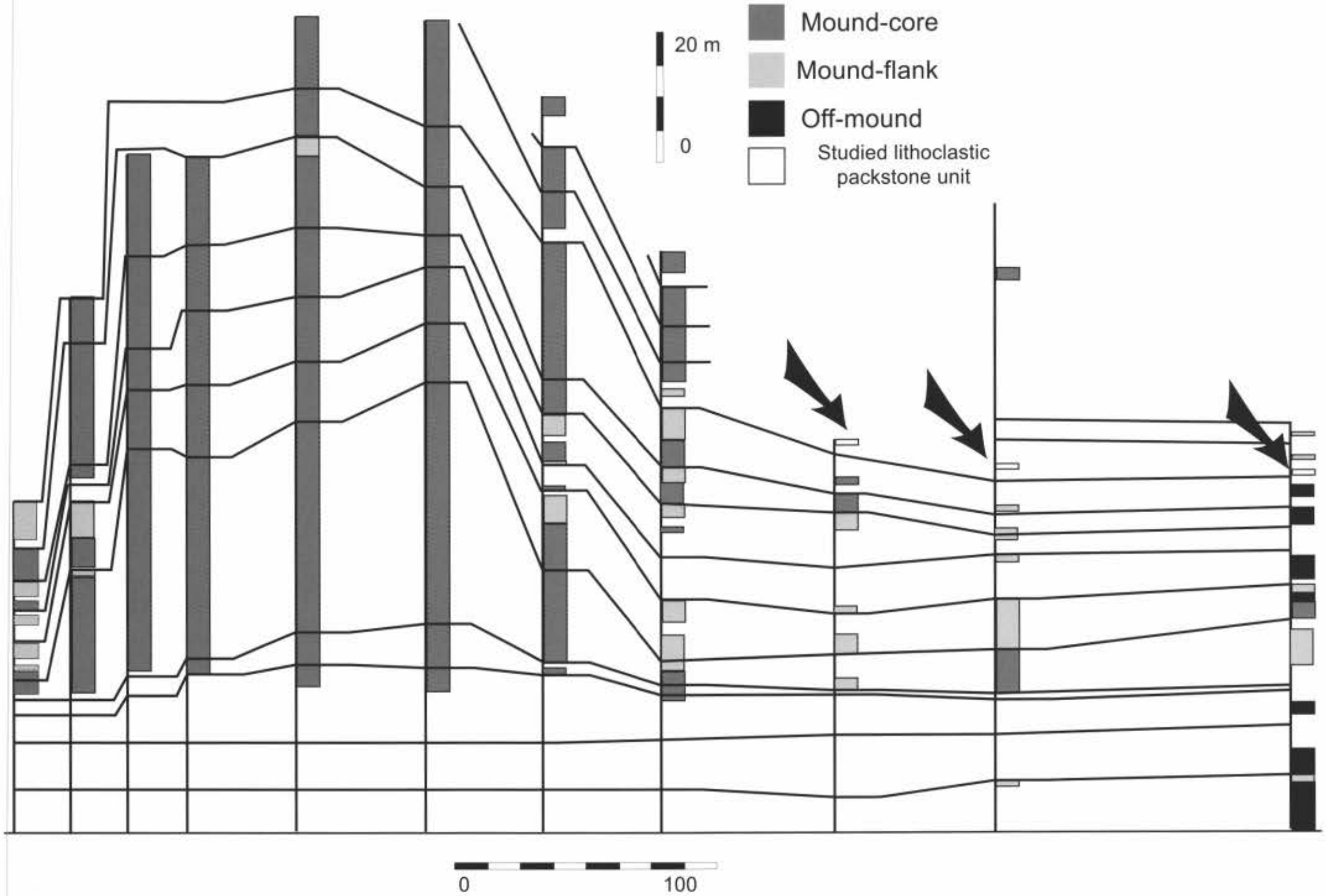

FIGURE 4. Stratigraphic relationship between lithoclastic packstone unit and mound core. (A) Outcrop photograph of phylloid algal mound in western Orogrande basin. Arrow indicates approximate position of lithoclastic packstone unit. (B) Stratigraphic sections measured through the mound system showing the stratigraphic distribution of mound-core (dark gray), mound-flank (light gray), and off-mound (black) facies with respect to sequence boundaries (solid lines). Arrows indicate the position of the lithoclastic packstone unit.

(3) recrystallized sparry calcite fans. All samples exhibit low Mg concentration (< 4 mol % $MgCO_3$, Tucker and Wright, 1990). Below, we make relative comparisons of elemental concentrations among the different cement types observed in the studied samples. See Table 1 for a summary of geochemical data.

Type-1: Radial-Fibrous Cementstone Facies

Radial-fibrous cements occur as small (3-10 mm diameter) abraded clasts exhibiting finely fibrous, apparent botryoidal texture that results in a sweeping or undulose extinction pattern in cross-polarized light (Figs. 5a,b). In plane-polarized light this cement is slightly pleochroic, ranging in color from light brown to brown, and consists of calcite crystals that exhibit elongation parallel to the c-axis. These crystals are of uniform width (< 25 µm), have a high length to width ratio (Sandberg, 1985), and nucleate outward from cores of cement spherules, resulting in a finely radial-fibrous, internal fabric. Crystal-tip terminations appear to be square or blunt at high magnification (Fig. 5c) imparting a characteristic "paintbrush" or "feathery" texture to the outer margins of the crystals (Folk and Assereto, 1976; Loucks and Folk, 1976). Solid inclusions of an Fe-rich phase (hematite, and magnetite and/or pyrrhotite) line concentric growth "bands" and are more concentrated near the cores of the cement spherules (Fig. 5d). Scanning electron microscopy (SEM) shows this phase to exhibit a felted, mesh-like habit (Fig. 5e).

Under cathodoluminescence (CL) these nonfossiliferous radial-fibrous cements exhibit a moderately uniform to slightly mottled, dull-red luminescence. Zones of bright-red luminescence appear to occupy areas of recrystallization, which in some instances occur adjacent to the more Fe-rich, non-luminescent, outer margin of the growth bands.

Microprobe analysis of the cements indicates low Fe (400 ppm ± 300), and Mn (450 ppm ± 350), elevated Mg (0.7 mole % $MgCO_3$, 8650 ppm ± 5400), and moderately elevated Sr concentration (1400 ppm ± 820). Local areas of elevated Fe (3190 ± 830) and Mn (2180 ppm ± 850), however, are present. Similarly, these Fe- and Mn-rich zones exhibit elevated Mg (4790 ppm ± 870) and moderately elevated Sr (1560 ppm ± 710).

Moderately elevated Sr (>1000 ppm), and blunt to square-tip crystal terminations indicate that these nonfossiliferous radial-fibrous cements are the product of neomorphism of former botryoidal aragonite (e.g., Kendall and Tucker, 1973; Cys and Mazzullo, 1977; Kendall, 1977; Mazzullo and Cys, 1979; Sandberg, 1985; Davies and Nassichuk, 1990; Sumner and Grotzinger, 2000). Locally high Fe concentrations, solid inclusions of Fe-rich minerals (i.e., hematite, and magnetite and/or pyrrhotite), and lack of biota suggest that these cements precipitated under relatively oxygen-poor conditions.

Type-2: Radial-Fibrous Cement in Boundstone Facies

Radial-fibrous cement occurs as fans between allochems (foraminfera, algae, etc.) in boundstone clasts (Fig. 6). In plane-polarized light this cement is slightly pleochroic, ranging in color from light brown to brown. Crystal-tip terminations are square or blunt at high magnification and the cement exhibits abundant sweeping extinction under cross-nichols similar to the type 1 cement. In contrast to type 1 cement, however, type 2 cements contain neither concentric growth "bands" nor solid inclusions of Fe-rich minerals. Under CL these cements are mottled dull-red to non-luminescent, but do contain areas of bright-red luminescence. Backscatter electron imaging reveals distinct zones of alternating higher and lower atomic mass that correspond to regions of high- and low-Mg concentrations as compared to the other cement types.

High-Mg zones are characterized by Mg > 4000 ppm with average Mg of 4560 ppm ± 250, low to moderate Fe (730 ppm ± 660) and variable Mn (2770 ppm ± 2000). Sr (620 ppm ± 210) is relatively depleted in these zones. Low-Mg (790 ppm ± 320) zones exhibit low Fe and Mn (both below detection limit) and high Sr (5900 ppm ± 260, maximum > 6000 ppm). Inclusions euhedral calcite (75 µm along long axis) within the fibrous cement were also analyzed and exhibit elevated Mg (8.5 mole % $MgCO_3$, 110,290 ppm ± 1,170). These crystals also show elevated Fe (4470 ppm ± 1,200) and Mn (1180 ppm ± 90), and an average Sr concentration of 1190 ppm ± 470.

The moderate to elevated Sr in both zones, blunt to square crystal-tip terminations, radial-fibrous morphology and finely-fibrous internal texture are consistent with an aragonitic precursor. The presence of high-Mg zones with low Sr also suggests the occurrence of high-Mg calcite. The abundant skeletal

TABLE 1. Summary of geochemical data.

Cement Type	Stratigraphic Context	Avg. Elemental Concentrations, ppm (std dev)				Fe mineral inclusions
		Mg	Sr	Fe	Mn	
Recrystallized Sparry Calcite Fans	In situ mound-core cementstone	1430 (390)	510 (300)	BDL	BDL	none
Nonfossiliferous, Radial-fibrous cement (type 1)	Clasts within mound-flank litho-clastic packstone	8650 (5400)	1400 (820)	400 (300)	450 (350)	present
Fossiliferous, Radial-fibrous cement (type 2)	Clasts within mound-flank litho-clastic packstone					none
High-Mg zones		4560 (250)	620 (210)	730 (660)	2770 (2000)	
Low-Mg zones		790 (320)	5900 (260)	BDL	BDL	
Recrystallized Sparry Calcite Fans (type 3)	Clasts within mound-flank lithoclastic packstone	550 (330)	5370 (650)	400 (300)	BDL	none

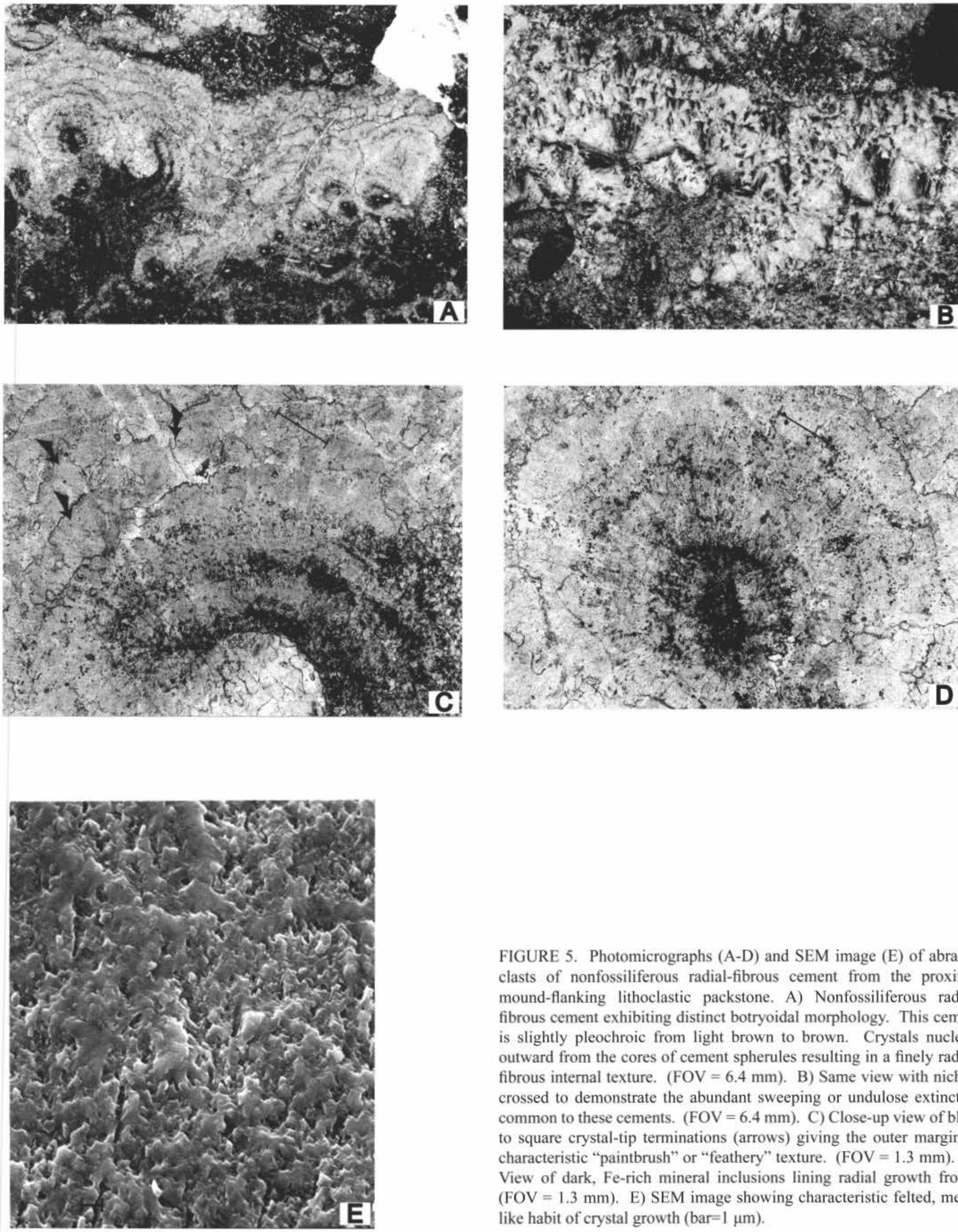

FIGURE 5. Photomicrographs (A-D) and SEM image (E) of abraded clasts of nonfossiliferous radial-fibrous cement from the proximal mound-flanking lithoclastic packstone. A) Nonfossiliferous radial-fibrous cement exhibiting distinct botryoidal morphology. This cement is slightly pleochroic from light brown to brown. Crystals nucleate outward from the cores of cement spherules resulting in a finely radial-fibrous internal texture. (FOV = 6.4 mm). B) Same view with nichols crossed to demonstrate the abundant sweeping or undulose extinction common to these cements. (FOV = 6.4 mm). C) Close-up view of blunt to square crystal-tip terminations (arrows) giving the outer margins a characteristic "paintbrush" or "feathery" texture. (FOV = 1.3 mm). D) View of dark, Fe-rich mineral inclusions lining radial growth fronts. (FOV = 1.3 mm). E) SEM image showing characteristic felted, mesh-like habit of crystal growth (bar=1 μm).

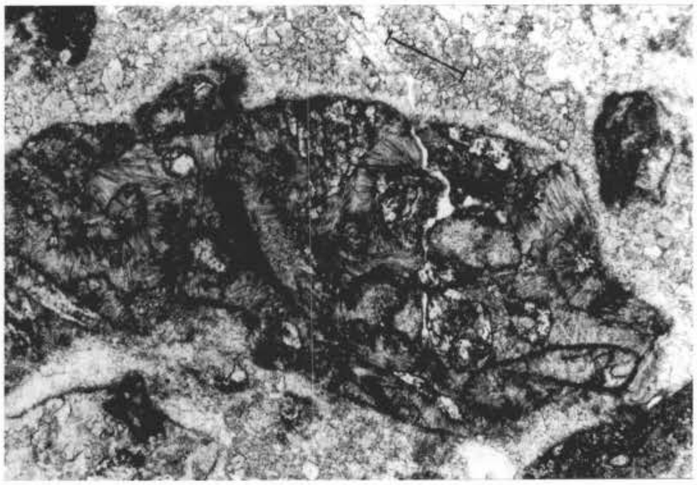

FIGURE 6. Photomicrograph of type-2 radial fibrous cement binding various allochems (foraminifera, algae, etc.) together in a grainstone. (FOV = 3.2 mm).

components incorporated within this cement type and lack of any Fe-rich growth bands support the inference that these were precipitated under relatively oxic conditions.

Type-3: Recrystallized Sparry Calcite Fans

Clasts of faintly radial-fibrous, recrystallized cement fans also occur within the lithoclastic packstone (Fig. 7a), and appear analogous to *in situ* cements observed within the mound core. These recrystallized cements are characterized by sparry calcite crystal mosaics that are colorless to light brown, and non-pleochroic. SEM images of these cements (Fig. 7b) reveal a blocky texture in contrast to the finely felted, mesh-like habit exhibited by the type 1 radial-fibrous cements (Fig. 5e). Under CL these lithoclasts are mostly non-luminescent, but do contain inclusions of bright red luminescent crystals.

These sparry calcite mosaics exhibit low to slightly variable concentrations of Fe (400 ppm $\pm$ 300), Mg (550 ppm $\pm$ 330), and Mn (BDL), but elevated Sr (5370 ppm $\pm$ 650). The differences observed between the chemistry of the *in situ* mound core cements and the recrystallized clasts of cements within the lithoclastic packstone could be related to differences in later diagenesis. The cements within the mound core underwent early, post-depositional diagenesis in very Sr-rich pore waters, owing to the abundance of aragonitic submarine cement and aragonitic biota (i.e. phylloid algae) within the system. Clasts of this cement were then eroded, transported and preserved within the lithoclastic packstone, while *in situ* cementstone in the mound core underwent further diagenesis (meteoric).

Rock Magnetism

Because each core taken from the lithoclastic packstone potentially incorporates several different cement clasts, magnetic results from alternating field demagnetization (AF), isothermal remanent magnetization (IRM), and triaxial decay are representative of the bulk rock rather than individual phases. These techniques shed some light on the presence and mineralogy of the Fe-rich phases that were observed only in the type 1 cement.

Alternating field (AF) demagnetization is a technique used to test for the presence of low-coercivity minerals such as magnetite and pyrrhotite (Butler 1998). Our samples subjected to AF demagnetization show a complete loss of magnetic intensity at 60 mT (Fig. 8). This indicates a magnetic contribution of a low-coercivity mineral such as magnetite and/or pyrrhotite.

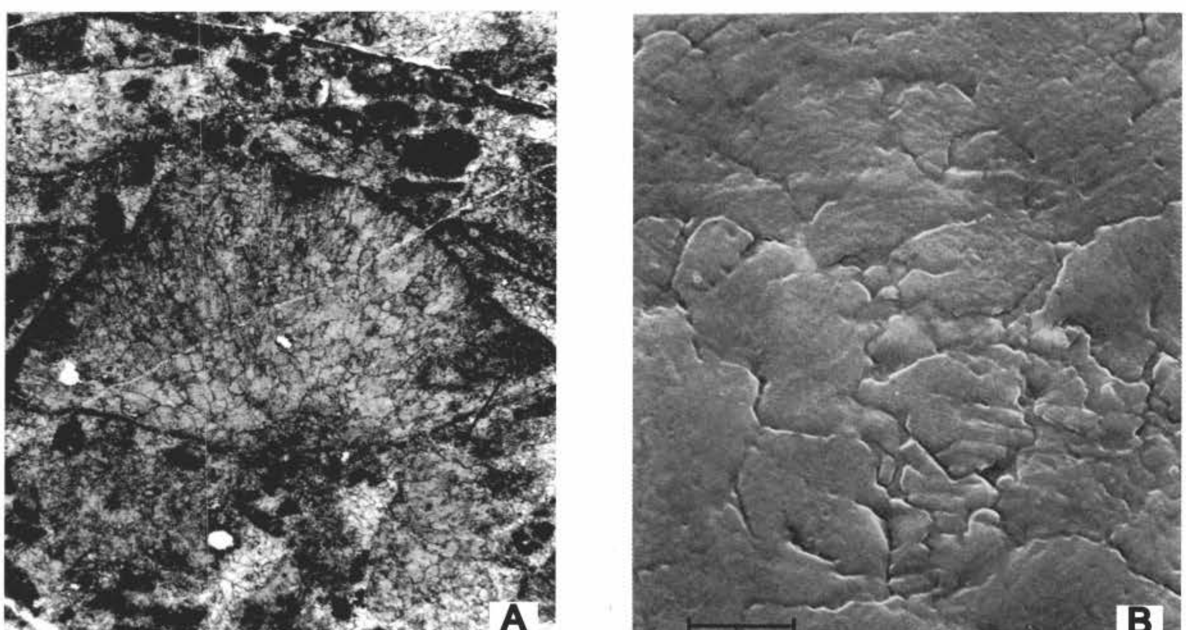

FIGURE 7. Recrystallized sparry calcite fan. A) Recrystallized botryoid exhibiting faint retention of relict fibrous structure. (FOV = 3.2 mm). B) SEM image showing characteristic blocky texture of calcite crystal mosaics (bar= 5μm).

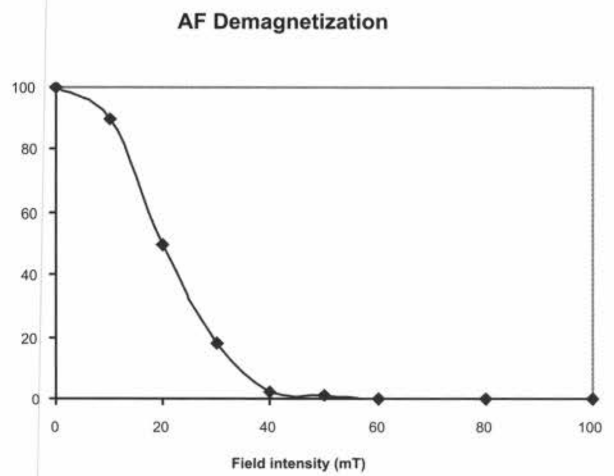

FIGURE 8. AF demagnetization showing complete loss of magnetic intensity at 60 mT, indicating the presence of a low-coercivity phase (magnetite and/or pyrrhotite).

Isothermal remanent magnetization (IRM) acquisition is the measure of the intensity of acquired magnetization when a sample is exposed to a magnetizing field at constant temperature. IRM acquisition, followed by triaxial decay (Lowrie 1990), is a test for the presence of both low- and high-coercivity phases. High-coercivity magnetic minerals (e.g. hematite) are not detectable with AF demagnetization as their coercive force easily exceeds the maximum available field during AF decay. Our data (Fig. 9) illustrate rapid acquisition of IRM at relatively low field intensities (0-350 mT), indicating the presence of a low-coercivity magnetic phase such as magnetite and/or pyrrhotite. At higher field intensities (> 350 mT) the IRM gradually increases indicating the presence of a high-coercivity phase (hematite). IRM acquisition was then followed by thermal decay of the three orthogonal directions (x-y-z directions) at 120 mT, 500 mT, and 2500 mT (Fig. 10). Triaxial decay (Lowrie, 1990) analysis allows for the evaluation of the relative importance of high- and low-coercivity phases in the sample. The gradual loss of magnetization at thermally distributed unblocking temperatures for field intensities of 120 mT and 500 mT indicates decay of low-coercivity magnetic material (magnetite and/or pyrrhotite), consistent with the results of AF demagnetization. The thermally discrete unblocking temperature of the 2500 mT curve, however, reflects the dominance of small (< 15 μm) high-coercivity grains of hematite.

Based on our analyses, we infer that the dominant magnetic carrier for bulk rock magnetization resides in hematite, with a minor contribution of magnetite and/or pyrrhotite. Petrographic and geochemical analyses of abraded clasts of submarine cements within the lithoclastic packstone indicate that only the type 1, nonfossiliferous, radial-fibrous cement contains solid inclusions of Fe-rich minerals. The rock-magnetic results thus indicate that these inclusions consist of magnetite and/or pyrrhotite together with hematite. The latter is likely an oxidation product of the former, perhaps a result of modern weathering.

DISCUSSION

Based on our analyses, the lithoclastic packstone contains abraded clasts of cement that have been eroded from different parts of the mound during a single glacioeustatic cycle. The varying chemistry and morphology of these different cements indicate that seawater chemistry fluctuated during cement pre-

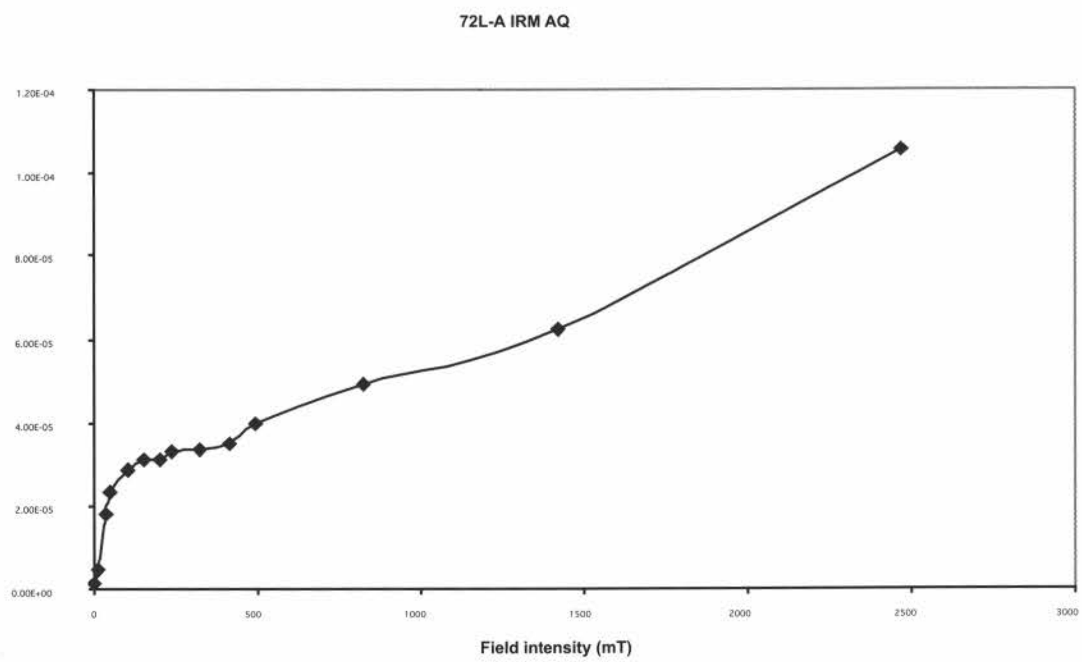

FIGURE 9. IRM acquisition plots. Rapid acquisition of IRM at relatively low field intensities (0-350 mT) is indicative of the presence of a low coercivity phase (magnetite and/or pyrrhotite). Gradual increase in IRM at higher field intensities (>350 mT) indicates the presence of a high coercivity phase (hematite).

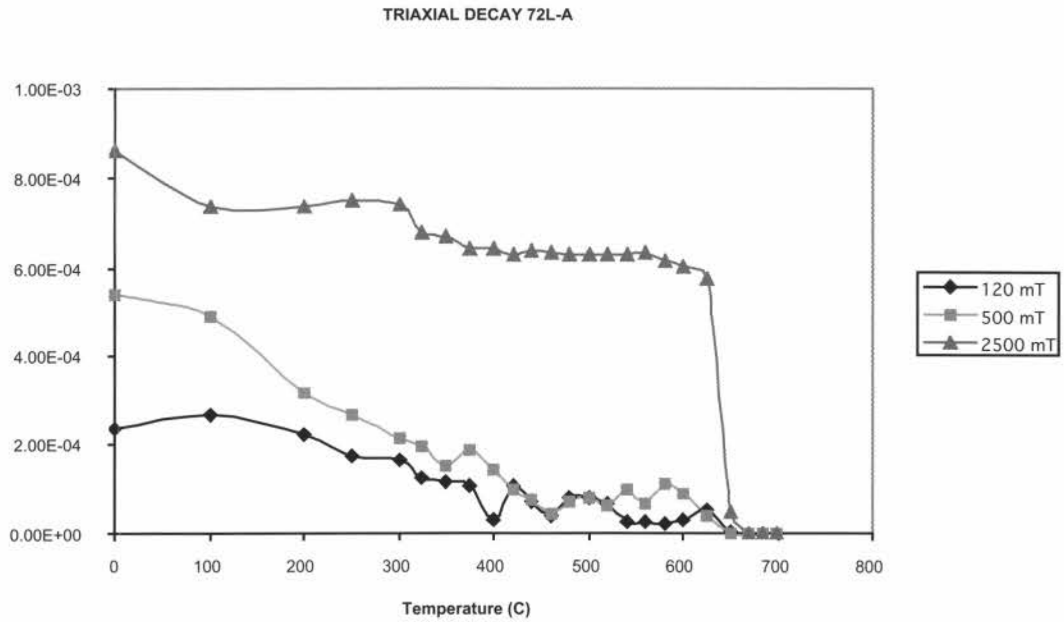

FIGURE 10. Triaxial decay plot showing gradual loss of magnetization at low field intensities indicating the presence of a low coercivity phase (magnetite and/or pyrrhotite). Thermally discrete unblocking temperature distribution at the 2,500 mT curve reflects the presence of hematite.

cipitation through a given glacioeustatic cycle. We infer that the radial-fibrous (type 1) cement is derived from mound-core cementstone, which typically occur in basal-middle positions of a glacioeustatic cycle (Soreghan and Giles, 1999a). The radial-fibrous (type 2) cement is derived from foraminiferal/algal boundstone facies, which typically occupy highstand positions within a glacioeustatic sequence (Soreghan and Giles, 1999a).

Type 1 radial-fibrous cement precipitated during early transgressive phases at least locally appears to reflect oxygen-poor conditions. This cement contains no macroscopic biota, and exhibits zones of locally elevated Fe. Solid inclusions of a Fe-rich phase define bands of crystal growth fronts. Geochemical analysis indicates these inclusions to be an iron sulfide. Further rock magnetic investigations reveal that these Fe-rich mineral inclusions to be magnetite and/or pyrrhotite, and hematite. The inference of low-oxygen conditions during early transgression is consistent with the model for early transgressive reflux dolomitization in the mound system as proposed by Soreghan et al. (2000). In this model, NFS dolomite originated by reflux of mesosaline to hypersaline brines associated with each glacioeustatic transgression. Soreghan and Giles (1999b) documented a minimum amplitude of 80-100 m in sea level fluctuation in the Orogrande basin, and coeval strata across the southern, western, and central Orogrande basin show evidence of basin restriction during lowstand (Kottlowski, 1960). These data record near-complete basin exposure during each glacioeustatic lowstand, and the pooling of mesosaline to hypersaline waters in restricted regions of the basin. NFS dolomite is Fe-rich and interpreted to have been precipitated in mesosaline water suggesting that seawater associated with early transgression was both briney and oxygen poor (Soreghan et al., 2000). This is consistent with our inference that type 1 radial-fibrous cement precipitated in relatively oxygen-poor conditions. The abundant biota associated with type 2 radial-fibrous cement, as well as lower Fe, and lack of any Fe-rich mineral inclusions indicate that this cement precipitated in relatively oxygen-rich waters during glacioeustatic highstand. From this, we infer that that seawater chemistry fluctuated from poorly oxygenated during early transgressive stages to well oxygenated late transgression to highstand stages.

CONCLUSIONS

(1) Type 1 radial-fibrous cementstone is volumetrically abundant in Upper Pennsylvanian phylloid algal bioherms in the western Orogrande basin, and commonly occupies basal transgressive parts of mound buildups (Soreghan and Giles, 1999a). Typically, recrystallized faintly fibrous calcite spar predominates within the mound system, however, abraded clasts of finely preserved fibrous submarine cement occur within a thin (>20 cm thick) lithoclastic packstone that is in the proximal mound-flank region.

(2) Three distinct submarine cement types are observed to occur as transported clasts within the lithoclastic packstone. Type 1 radial-fibrous cement contains elevated Sr, exhibits blunt to square crystal-tip terminations, and contains solid inclusions of hematite and magnetite and/or pyrrhotite concentrated along radial growth bands. Type 2 radial-fibrous cement also exhibits blunt to square crystal-tip terminations, lack any Fe-rich mineral inclusions and growth bands, and nucleate directly off of skeletal components. These cements are compositionally zoned with areas of higher and lower concentrations of Mg. Recrystallized sparry calcite fans consist of recrystallized calcite mosaics that faintly preserve former radial-fibrous morphology, and contain elevated and low Mg.

(3) Bulk-rock magnetic data indicate a magnetic contribution of hematite, and magnetite and/or pyrrhotite. The type 1 radial-fibrous cement is the only phase that contains solid inclusions of

Fe-rich minerals, and exhibits variable but locally high Fe (3190 ppm $\pm$ 830).

(4) All three cement types represent neomorphism of formerly aragonitic submarine cements. We infer that the variable chemistry of the well-preserved phases reflects precipitation under conditions of fluctuating seawater chemistry, and through a single glacioeustatic cycle. The lack of biota and the presence of solid inclusions of Fe-rich phases in addition to locally elevated trace elemental Fe suggest that type 1 radial-fibrous cements precipitated in relatively oxygen-poor conditions during early transgression. The incorporation of biota and the lack of any Fe-rich mineral inclusions or growth bands imply that the type 2 radial-fibrous cement precipitated in oxygen-rich conditions during highstand when conditions were favorable for supporting organisms.

ACKNOWLEDGMENTS

Acknowledgment is made to the donors of The Petroleum Research Fund (ACS-PRF # 31893-G8 and # 35217-AC8 to GSS), administered by the American Chemical Society, for partial support of this research. We gratefully acknowledge R. Myers (Range Geologist, Environmental Stewardship Division) and T.A. Ladd (Director, Environment and Safety Directorate, U.S. Army White Sands Missile Range) for arrangement of range visitation. Many thanks to John Dodds, Patrick Doherty, and Briann Zimmermann for invaluable field assistance. Analytical and technical support at the University of Oklahoma was provided by Ron Conlon (XRD), George Morgan (microprobe), and Raleigh Blumstein, Jamie Foucher, Angela Miller (rock magnetics). We wish to thank S. Carpenter, G. Davies, R. Folk, B. Kirkland, S. Mazzullo, C. Moore, J. Pigott, and J.Wilson for discussions that stimulated our thinking on submarine cement and their diagenesis. This manuscript benefited greatly by the careful reviews of S. Carpenter, G. Wahlman, and two anonymous reviewers. This paper was approved for public release by White Sands Missile Range; distribution unlimited. OPSEC review completed on May 8, 2002.

REFERENCES

Assereto, R., and Folk, R.L., 1980, Diagenetic fabrics of aragonite, calcite, and dolomite in ancient peritidal-spelean environment: Triassic Calcare Rosso, Lombardia, Italy: Journal of Sedimentary Geology, v. 50, p. 371-394.

Bathurst, R.G.C., 1959, The cavernous structure of some Mississippian Stromatactis reefs in Lancashire, England: Journal of Geology, v. 67, p. 506-521.

Butler, R.F., 1998, Paleomagnetism: Magnetic Domains to Geologic Terranes: Boston, Blackwell Scientific Publications, 319 p.

Cys, J.M., and Mazzullo, S.J., 1977, Biohermal submarine cements, Laborcita Formation (Permian), northern Sacramento Mountains, New Mexico, *in* Butler, J.H., ed., Geology of the Sacramento Mountains, Otero County, New Mexico: West Texas Geological Society, Publication 1977-68; 43-48.

Davies, G.R., 1977, Former magnesian calcite and aragonite submarine cements in upper Paleozoic reefs of the Canadian Arctic: A summary: Geology, v. 5 p. 11-15.

Davies, G.R., and Nassichuk, W.W., 1990, Submarine cements and fabrics in Carboniferous to Lower Permian, reefal, shelf margin and slope carbonates, northwestern Ellesmere Island, Canadian Arctic Archipelago: Geological Survey of Canada Bulletin, v. 399, 77 p.

Dickson, J.A.D., 1965, A modified staining technique for carbonates in thin section: Nature, v. 205, p. 587.

Doherty, P.D., Soreghan G.S., and Castagna, J.P., 2002, Outcrop-based reservoir characterization: A phylloid algal mound, western Orogrande basin (New Mexico): American Association of Petroleum Geologists Bulletin.

Folk, R.L., and Assereto, R., 1976, Comparative fabric of length-slow and length-fast calcite and calcitized aragonite in a Holocene speleothem, Carlsbad Caverns, New Mexico: Journal of Sedimentary Petrology, v. 46, p. 486-496.

Goldstein, R.H., 1988, Cement stratigraphy of Pennsylvanian Holder Formation, Sacramento Mountains, New Mexico: American Association of Petroleum Geologists Bulletin, v.72, p. 425-438.

Gordon, I.T., 1997, The effect of relative sea-level change on the development of phylloid algal bioherms Laborcita Formation (Lower Permian), Sacramento Mountains, New Mexico [M. S. Thesis]: Austin, University of Texas, 88 p.

Grotzinger, J.P., and Knoll, A.H., 1995, Anomalous carbonate precipitates: Is the Precambrian the key to the Permian?: Palaios, v. 10, p. 578-596.

Kendall, A.C., and Tucker, M.E., 1973, Radiaxial fibrous calcite: A replacement after acicular carbonate: Sedimentology, v. 20, p. 365-389.

Kendall, A.C., 1977, Fascicular-optic calcite: A replacement of bundled acicular carbonate cements: Journal of Sedimentary Petrology, v. 47, p. 1056-1062.

Kimbell T.N., and Humphrey J.D., 1994, Geochemistry and crystal morphology of aragonite cements of mixing-zone origin: Journal of Sedimentary Research, v. 64 p. 604-614.

Kottlowski, F.E., Flowers, R.H., and Thompson, M.L., 1956, Stratigraphic studies of the San Andres Mountains, New Mexico: New Mexico Bureau of Mines and Mineral Resources Memoir v. 1, 132 p.

Kottlowski, F.E., 1960, Depositional features of the Pennsylvanian of south-central New Mexico. *in* Kottlowski, F.E., Foster, R.W., Harbour, R.L., and Nelson, L.A., eds., Guidebook for the Northern Franklin Mountains and the Southern San Andres Mountains with emphasis on Pennsylvanian Stratigraphy: Roswell Geological Society Guidebook, p. 96-130.

Loucks, R.G., and Folk, R.L., 1976, Fan-like rays of former aragonite in Permian Capitan Reef pisolite: Journal of Sedimentary Petrology, v. 46, p. 483-485.

Lowrie, W., 1990, Identification of ferromagnetic minerals in a rock by coercivity and unblocking temperature properties: Geophysical Research Letters, v. 17, p. 159-162.

MacKenzie, F.T., and Pigott, J.D., 1981, Tectonic controls of Phanerozoic sedimentary rock cycling: Journal of the Geological Society of London, v. 138, p. 1075-1084.

Mazzullo, S.J., and Cys, J.M., 1979, Marine aragonite sea-floor in Permian phylloid algal Mounds, Sacramento Mountains, New Mexico: Journal Sedimentary Petrology, v. 49, p. 917-936.

Nelson, G.S., and James, N.P., 2000, Marine cements in mid-Tertiary cool-water shelf limestones of New Zealand and southern Australia: Sedimentology, v. 47, p. 609-629.

Otte, C. Jr, and Parks, J.M., 1963, Fabric studies of Virgil and Wolfcamp bioherms, New Mexico: Journal of Geology, v. 71, p. 380-396.

Plumley, W.J., and Graves, R.W. Jr., 1953, Virgilian reefs of the Sacramento Mountains, New Mexico: Journal of Geology, v. 61, p. 1-16.

Pol, J.C., 1982, Sedimentation and diagenesis of an Upper Pennsylvanian (Virgilian) mixed carbonate-clastic sequence, Hueco Mountains, El Paso County, west Texas [M. S. Thesis]: Austin, University of Texas, 212 p.

Pol, J.C., 1985, Sedimentation of and Upper Pennsylvanian (Virgilian) phylloid algal mound, Hueco Mountains, El Paso County, west Texas *in* Toomey, D.F., and Nitecki, M.H., eds., Paleoalgology, Contemporary Research and Applications: Springer-Verlag, Berlin, p. 188-207.

Rahnis, M.A., and Kirkland, B.L., 1999, Distribution, petrography, and geochemical characterization of radiaxial calcite and associated diagenetic events in the Capitan Formation, west Texas and New Mexico *in* Saller, A.H., Harris, P.M., Kirkland, B.L., and Mazzullo, S.J. eds., Geologic Framework of the Capitan Reef: Society of Economic Paleontologists and Mineralogists Special Publication, v. 65, p. 175-191.

Sandberg, P.A., 1983, An oscillating trend in Phanerozoic non-skeletal carbonate mineralogy: Nature, v. 305, p. 19-22.

Sandberg, P., 1985, Aragonite cements and their occurrence in ancient limestones *in* Schneidermann, N., and Harris, P.M, eds., Carbonate Cements: Society of Economic Paleontologists and Mineralogists Special Publication, v. 36, p. 33-57.

Schoderbek, D.A., 1994, Environments of deposition and patterns of cyclicity of the Panther Seep Formation, southern San Andres Mountains *in* Garber, R.A., and Keller, D.R. eds., Field Guide to the Paleozoic Section of the San Andres Mountains: Society of Economic Paleontologists and Mineralogists

Publication No. 94-35, p. 87-103.

Shinn, E.A., 1969, Submarine lithification of Holocene carbonate cements in the Persian Gulf: Sedimentology, v. 12, p. 109-144.

Soreghan, G.S., 1994, Stratigraphic responses to geologic processes: Late Pennsylvanian eustasy and tectonics in the Pedregosa and Orogrande basins, Ancestral Rocky Mountains: Geological Society of America Bulletin, v. 106, p. 1195-1211.

Soreghan, G.S., and Giles, K.A., 1999a, Facies character and stratal responses to accommodation in Pennsylvanian bioherms, western Orogrande basin, New Mexico: Journal of Sedimentary Research, v. 69, p. 893-908.

Soreghan, G.S., and Giles, K.A., 1999b, Amplitudes of Late Pennsylvanian glacioueustasy: Geology, v. 27, p. 255-258.

Soreghan, G.S., Engel, M.H., Furley, R.A., and Giles, K.A., 2000, Glacioeustatic transgressive reflux: stratiform dolomite in bioherms of the western Orogrande basin, New Mexico: Journal of Sedimentary Research, v. 70, p. 1315-1332.

Stoklosa, M.L., Simo, J.A., and Wahlman, G.P., 1998, Facies description and evolution of a Wolfcampian (Early Permian) shelf margin: Hueco Mountains, West Texas: New Mexico Geological Society Guidebook, v. 49, p. 177-186.

Sumner, D.Y., and Grotzinger, J.P., 2000, Late Archean aragonite precipitation: petrography, facies associations, and environmental significance *in* Grotzinger, J.P., and James, N.P., eds., Carbonate Sedimentation and Diagenesis in the Evolving Precambrian World: Society of Economic Paleontologists and Mineralogists Special Publication, v. 67, p. 3-20.

Toomey, D.F., Wilson, J.L., and Rezak, R., 1977, Evolution of Yucca Mound complex, Late-Pennsylvanian phylloid-algal buildup, Sacramento Mountains, New Mexico: American Association of Petroleum Geologists Bulletin, v. 61, p. 2115-2133.

Toomey, D.F., and Babcock, J.A., 1983, Precambrian and Paleozoic algal carbonates, West Texas-southern New Mexico: Colorado School of Mines Professional Contribution, no. 11, 345 p.

Tucker, M.E., and Wright, V.P., 1990, Carbonate Sedimentology: Oxford, Blackwell Science, 482 p.

Wahlman, G.P., 1985, Lower Permian (Wolfcampian) Archaeolithoporella-Tubiphytes-Sponge boundstones from the subsurface of West Texas *in* Toomey, D.F., and Nitecki, M.H., eds., Paleoalgology, Contemporary Research and Applications: Springer-Verlag, Berlin, p. 208-215.

Wahlman, G.P., 1988, Subsurface Wolfcampian (Lower Permian) shelf-margin reefs in the Permian basin of west Texas and southeastern New Mexico: SEPM, Midcontinent Section, Special Publication, 1, p. 177-204.

Wahlman, G.P., Tasker, D.R., St. John, J.W., and Werle, K.J., 1992, Shelf-margin bioherms and associated facies in the Lower Permian Hueco Group (Late Wolfcampian), Hueco Mountains, West Texas: Geological Society of America, Annual Meeting, Abstracts with Programs, v. 24, p. 109.

Wendt, J., 1977, Aragonite in Permian Reefs: Nature, v. 267, p. 335-337.

Wilson, J.A., 1977, Regional distribution of phylloid algal mounds in late Pennsylvanian and Wolfcampian strata of southern New Mexico *in* Butler, J.H., ed., Geology of the Sacramento Mountains, Otero County, New Mexico: West Texas Geological Society Publication 1977-68, p. 1-7.

Woods, A.D., Bottjer, D.J., Mutti, M., and Morrison, J., 1999, Lower-Triassic large sea-floor carbonate cements: Their origin and a mechanism for the prolonged biotic recovery from the end-Permian mass extinction: Geology, v. 27, p. 645-648.

Wray, J.L., 1962, Pennsylvanian algal banks, Sacramento Mountains, New Mexico *in* Geoeconomics of the Pennsylvanian Marine Banks in Southeast Kansas: Kansas Geological Society, 27th Field Conference, Guidebook, p. 129-133.

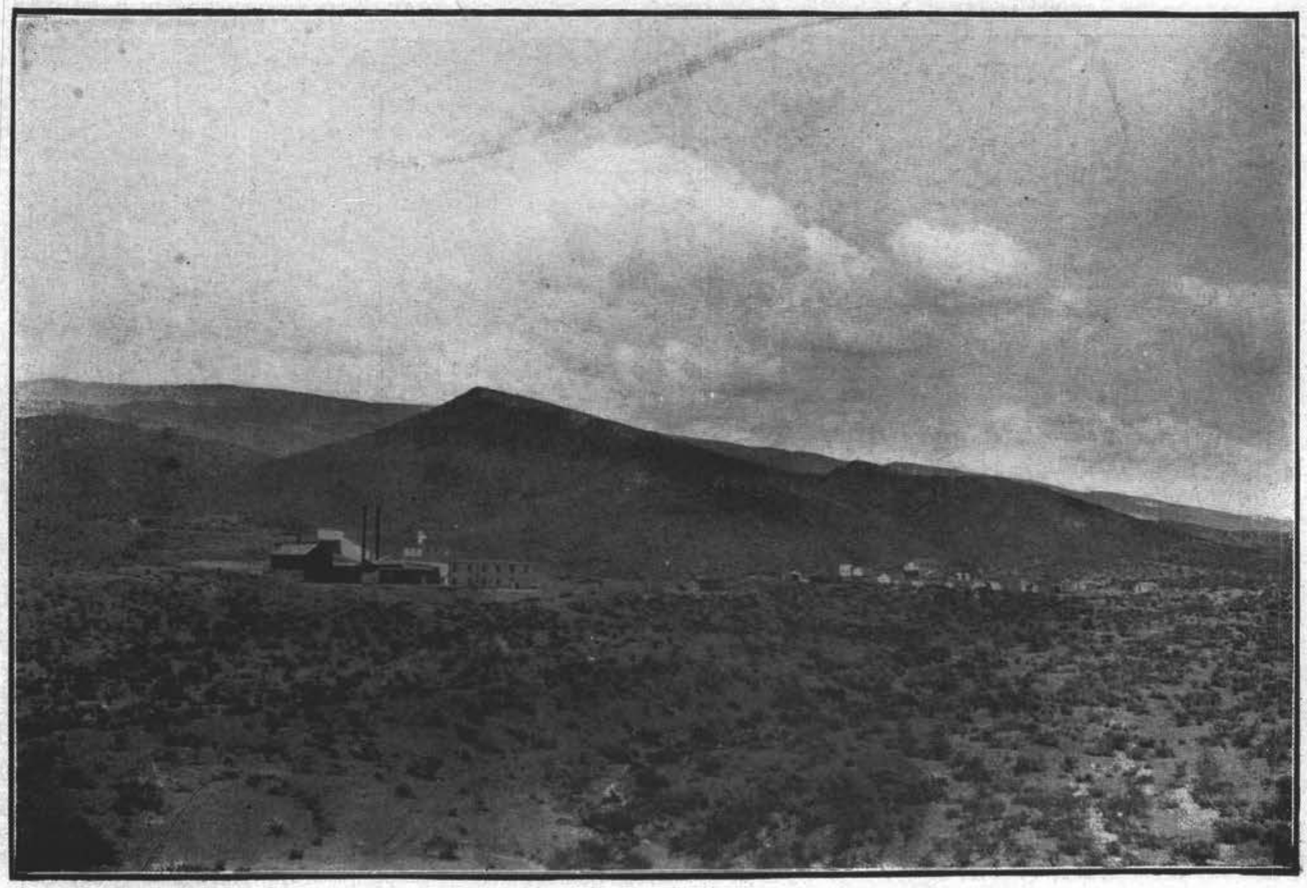

BIRD'S-EYE VIEW OF COMPANY'S PROPERTY AT ESTEY CITY

"Bird's Eye View of Estey City" from the Dividend Mining & Milling prospectus (1905) – courtesy Robert W. Eveleth.